Published in final edited form as:

Cytoskeleton (Hoboken). 2016 May ; 73(5): 246–257. doi:10.1002/cm.21298.

Disassembly of Myofibrils and Potential Imbalanced Forces on Z-Discs in Cultured Adult Cardiomyocytes

Honghai Liu[1], **Wan Qin**[2], **Zhonghai Wang**[2], **Yonghong Shao**[3], **Jingcai Wang**[1], **Thomas K. Borg**[4], **Bruce Z. Gao**[2], and **Meifeng Xu**[1,*]

[1]Department of Pathology and Laboratory Medicine, University of Cincinnati Medical Center, Cincinnati, Ohio 45267

[2]Department of Bioengineering and COMSET, Clemson University, Clemson, South Carolina 29634

[3]Key Laboratory of Optoelectronic Devices and Systems of Ministry of Education and Guangdong Province, College of Optoelectronic Engineering, Shenzhen University, Shenzhen 518060, China

[4]Department of Regenerative Medicine and Cell Biology, Medical University of South Carolina, Charleston, South Carolina 29425

Abstract

Myofibrils are the main protein structures that generate force in the beating heart. Myofibril disassembly is related to many physiological and pathological processes. This study investigated, in a cultured rat adult cardiomyocyte model, the effect of force imbalance on myofibril disassembly. The imbalance of forces that were exerted on Z-discs was induced by the synergistic effect of broken intercalated discs and actin–myosin interaction. Cardiomyocytes with well-preserved intercalated discs were isolated from adult rat ventricles. The ultrastructure of cardiomyocyte was observed using a customized two-photon excitation fluorescence and second harmonic generation imaging system. The contraction of cardiomyocytes was recorded with a highspeed CCD camera, and the movement of cellular components was analyzed using a contractile imaging assay technique. The cardiomyocyte dynamic remodeling process was recorded using a time-lapse imaging system. The role of actin–myosin interaction in myofibril disassembly was investigated by incubating cardiomyocytes with blebbistatin (25 μM). Results demonstrated that the hierarchical disassembly process of myofibrils was initiated from cardiomyocyte free ends where intercalated discs had broken, during which the desmin network near the free cell ends was destroyed to release single myofibrils. Analysis of force (based on a schematic model of cardiomyocytes connected at intercalated discs) suggests that breaking of intercalated discs caused force imbalance on both sides of the Z-discs adjacent to the cell ends due to actin–myosin interaction. The damaged intercalated discs and actin–myosin interaction induced force imbalance on both sides of the Z-discs, which played an important role in the hierarchical disassembly of myofibrils.

*Address correspondence to: Meifeng Xu, Department of Pathology and Laboratory Medicine, University of Cincinnati Medical Center, Cincinnati, Ohio 45267. meifeng.xu@uc.edu.

Additional Supporting Information may be found in the online version of this article.

Keywords

disassembly of myofibrils; imbalanced force; Z-disc; intercalated disc; cardiomyocyte

Introduction

Contraction of cardiac muscles is achieved by a hierarchical contractile structure. Sarcomeric components, that is, actin filaments and myosin filaments, assemble and are serially connected through Z-discs to form single myofibrils. Myofibrils are laterally bound together by desmin to form myofibril bundles. Integrity of myofibrils is critical to cardiomyocyte performance of the contractile function associated with cardiac muscle [Sequeira et al., 2014]. Disassembly of myofibrils, that is, detachment of sarcomeric proteins from mature myofibrils, is related to physiological [Ahuja et al., 2004] and pathological [Nishii et al., 2008] processes during heart development. Several factors have been found to induce disassembly of myofibrils such as myristate acetate [Lin et al., 1987] and those that stimulate proliferation of cardiomyocytes [Engel et al., 2005].

It is well established that cardiomyocytes are mechanically coupled through intercalated discs, which are important in regulating the myofibril structure of the connected cells [Simpson et al., 1993]. Damaged intercalated discs are related to heart diseases such as arrhythmogenic right ventricular cardiomyopathy (ARVC) [McKoy et al., 2000] and hypertrophic cardiomyopathy [Sepp et al., 1996]. ARVC, characterized by a high incidence of serious ventricular tachyarrhythmia and sudden cardiac death [Saffitz, 2011], has drawn wide attention since an investigation of sudden death among young people [Thiene et al., 1988]. It has also been reported that mutation of several intercalated disc proteins is associated with ARVC [Saffitz, 2011].

The study reported here investigated the role of intercalated discs in the disassembly of myofibrils. We employed a customized two-photon excitation fluorescence-second-harmonic generation (TPEF-SHG) hybrid imaging system to observe the disassembly of myofibrils in cultured adult rat cardiomyocytes. The dynamic remodeling process of the cardiomyocytes was recorded using a time-lapse imaging system. The contraction of cardiomyocytes was recorded with a high-speed CCD camera, and the local movement of the cardiomyocytes was analyzed using contractile imaging assay (CIA) techniques. Our study establishes correlations among the potential force imbalance on both sides of Z-discs induced by the broken or damaged intercalated discs and the actin–myosin interaction, and the hierarchical disassembly of myofibrils.

Results

Disassembly of Myofibrils Initiated from Cell Ends in Cultured Cardiomyocytes

Cardiomyocytes isolated from adult rat ventricle were classified into three morphological categories according to the ratio of their length to width (L/W): long rod shape (LRS, L/W>3), short rod shape (SRS, 2<L/W<3), and round shape (RS, L/W < 2). Freshly isolated cardiomyocytes typically were of LRS morphology. After 24 h in culture, several

cardiomyocytes were transformed into SRS. After 4 Days in culture in medium containing 20% fetal bovine serum (FBS), their morphology had transformed to RS (Fig. 1).

Cardiomyocytes were labeled with α-actinin and myosin heavy chain (MyHC) to investigate the disassembly of filaments. Images were captured using a TPEF-SHG imaging system. Previous research has indicated that SHG signals from cardiomyocytes arise from the coiled-rod structure of myosin filaments [Plotnikov et al., 2006]. In LRS cardiomyocytes, striated patterns of α-actinin and MyHC were clearly distinguishable in whole cells (Figs. 2A and 2B). However, in SRS cardiomyocytes, detachment of α-actinin and myosin filaments (SHG signal) first appeared at the cell ends (Figs. 2C and 2D). Data showed that 95.8% (23/24) had a weakened SHG signal in the cell ends. This was significantly higher than that obtained from LRS cardiomyocytes (52/65 = 80.6%). However, the α-actinin and MyHC signals were still strong at the cell ends. When cardiomyocytes transformed into RS, all striated myofibrillar patterns disappeared, α-actinin relocated to the cell periphery (90.7%, 78 of 86 arbitrarily selected cells), and myosin molecules randomly aggregated (Figs. 2E and 2F). The expression level of α-actinin and MyHC in cultured cardiomyocytes was semi-quantitated using Western blot and was significantly decreased in the cardiomyocytes cultured for 4 Days compared to those cultured for 1 Day (Fig. 2G).

Single Myofibril Release from Myofibril Bundles Was Initiated from Cell Ends

Desmin, a type III intermediate filament, plays a critical role in maintaining the structure of muscle cells [Bar et al., 2004]. Desmin patterns were observed in the different stages of disassembly to investigate the detachment of myosin filaments. The striated desmin became more randomly distributed inside the peanut-shape cardiomyocyte and was aggregated in the round-shape cell (Fig. 3A). In addition, the overlapping striated patterns of α-actinin and desmin show that the expression of α-actinin and desmin became mismatched at the cell ends when LRS cardiomyocytes transformed into SRS cardiomyocytes (Figs. 3B and 3C). This phenomenon implies that the detachment of the desmin network started from Z-discs and that single myofibrils were released from myofibril bundles.

The release of single myofibrils during contraction of cardiomyocytes was then further investigated. Supporting Information Video 1 shows that the movement of myofibrils in an LRS cardiomyocyte was highly synchronized. However, the synchronization of contraction among neighboring myofibrils no longer existed in the cells with loose lateral connections between myofibrils at the ends (Supporting Information Video 2), indicating that the connection of neighboring myofibrils could be broken prior to the loss of contractile capability. The movement of the myofibrils was further analyzed at the cell ends in Supporting Information Videos 1 and 2 using CIA (Figs. 4A and 4B, respectively). The direction of movement of the cardiomyocyte components are indicated by the colored arrows; the distance of the movements between snapshots (time intervals: 71 ms) is indicated by different colors and sizes of arrows (see the color bar below) (Supporting Information Video 1). Cellular components at the same cell end moved in the same direction before myofibril disassembly (Fig. 4A). However, when single myofibrils were released from the laterally bound myofibril bundles (Fig. 4B) (Supporting Information Video 2), movement of the cell components was uncoupled.

Actin-Myosin Interaction Is Necessary to Myofibril Disassembly

Cardiomyocyte shape and size are related to relaxed and contracted lengths. Actin–myosin interaction plays a critical role in regulating contraction of cardiomyocytes. Inhibition of actin–myosin interaction with blebbistatin (25 lM) significantly delayed the transformation of cardiomyocytes from LRS-to-RS (Figs. 5A and 5B). Relocation of α-actinin to the cell periphery and randomly distributed aggregation of desmin were also significantly repressed after actin–myosin interaction was inhibited (Figs. 5C and 5D).

Broken Intercalated Discs Promote Myofibril Disassembly

By using our modified adult cardiomyocyte isolation protocol, 2% of intercalated disc-connected cardiomyocytes were obtained. Cardiomyocyte contraction was not affected by the intercalated discs in freshly isolated cells with well-preserved intercalated discs (Figs. 6A and 6B) (Supporting Information Video 3, 4). Tight coupling of the cells at the intercalated discs was also observed using the CIA-visualized local displacement fields. The displacement intensity was propagated smoothly from one cardiomyocyte through the well-preserved intercalated discs to another cardiomyocyte during cell contraction (Figs. 6A and 6B). In contrast, the displacement intensity was not propagated from one cell to the other (Fig. 6C, Supporting Information Video 5) in cardiomyocytes with damaged intercalated disc.

Intercalated discs were localized by staining cardiomyocytes with connexin 43 and plakoglobin to distinguish the structure of filaments. It was observed that the striated α-actinin and desmin pattern near the intercalated discs was clearer than those with free ends. Shrinkage was delayed in cardiomyocytes with an end-to-end connection (Figs. 6D and 6E).

Real-time video microscopy inside an incubator recorded that cardiomyocytes with free cell ends transformed into a peanut shape in a shorter time than did cells connecting other cells through intercalated discs (Figs. 7A–7C). However, the inhibitor of actin–myosin interaction blebbistatin (25 μM) kept the cells with free ends in a LRS status (Fig. 7D).

Discussion

By employing several state-of-the-art techniques, the roles of intercalated discs and actin–myosin interaction on the disassembly of cultured adult rat cardiomyocytes were studied. Our results indicate that: (1) Isolated adult rat cardiomyocytes quickly disassembled expressed a morphology transformation from LRS to RS. The disassembly of myofibrils was started from the free ends of cell. (2) The integrity of intercalated discs and the interaction between myosin and actin play a critical role in disassembly of myofibrils. (3) Broken intercalated discs induced a potential force imbalance on both sides of the Z-discs adjacent to the cell ends, and which was enhanced by actin–myosin interaction.

Myofibril Disassembly Is Associated with Intercalated Discs and Actin-Myosin Interaction

Myofibrial disassembly resulted in the transformation of cardiomyocytes from LRS to RS. Messerli et al. [1993] reported that adult rat cardiomyocytes change their shape from elongated to round and that their myofibrils are disassembled upon culture in high

concentration fetal calf serum [Messerli et al., 1993]. Our study adds to this by a correlation of alpha-actinin, desmin, and myosin localization with SHG, which can be used to visualize the myosin rods, over the first days in culture. It has been indicated that the peanut shape is most likely due to the resorption of cell-cell contact structures at the intercalated discs with gap junctions disappearing first [Kostin et al., 1999]. Intercalated discs have been reported to play roles in regulating and stabilizing myofibril structure [Atherton et al., 1986]. However, the role of intercalated discs in the initialization and progress of the myofibril disassembly is still unclear.

We, here, investigated a progressive, hierarchical process of myofibril disassembly using isolated adult cardiomyocytes with well-preserved intercalated discs. Our study indicates that cardiomyocytes with well-preserved intercalated discs can maintain a LRS for an extended time in culture. Inhibition of actin–myosin interaction using blebbistatin not only preserved cell morphology in single cell culture but also prevented shrinkage of the free end of cardiomyocytes connected by intercalated discs. Our results are consistent with previous reports that myofibril disassembly first appears at the cell ends and then extends to the whole cell [Liu et al. 2013b]

Usually, samples of cardiomyocytes with integral intercalated discs are obtained from slices of the myocardium [Asimaki et al., 2009]. However, slices from fixed tissue are not good samples for studying dynamic changes of the intercalated discs. It has also been reported that intercalated discs can be rebuilt between cultured cells [McCain et al., 2012]. It is questionable whether rebuilt intercalated discs can faithfully reproduce their in vivo structure and function [Eppenberger and Zuppinger 1999; Zhou et al. 2013]. Therefore, isolating cardiomyocytes with intact intercalated discs directly from heart tissue could be beneficial for research.

Disassembly of Myofibrils Is Initiated from the Free End of Cells

It is well-accepted that changes in cardiomyocytes begin at the free cell ends. It has also been established that the morphological change of cells is usually dependent on two competitive physical molecular processes, including elongation and shortening of cells. The factors involved with elongating cardiomyocytes originate both inside and outside the cells. Inside the cell, sarcomeres extend themselves by pushing Z-discs outward after myosin detaches the actin filaments [Helmes et al., 1996; Previs et al., 2012]. Another factor comes from neighboring cells, which pull at the ends of the contracting cell. Our results suggest that the pulling effect of the neighboring cardiomyocytes played a major role in preventing shrinkage of cardiomyocytes with well-preserved intercalated discs. In contrast, actin–myosin interaction (inside the cell) shortens the sarcomeres and promotes shrinkage of the cells. When actin–myosin interaction is inhibited, cardiomyocyte shrinkage is prevented. The effects of the pull by the neighboring cardiomyocytes and the actin–myosin interaction inside the cell are in balance while the intercalated discs are well-preserved. The balance will be broken if the intercalated discs are damaged or if the pulling by the neighboring cardiomyocytes is partially or totally removed.

In this study, sarcomeric structure was observed under our lab-built TPEF-SHG imaging system using a procedure similar to that used in our previous report [Liu et al., 2013a].

TPEF provided higher quality images than conventional fluorescence techniques because of using the nonlinear interaction between near-infrared pulse laser and (intrinsic or labeled) fluorophores in tissues. The images obtained from the SHG are generated through the non-absorptive interaction of photons, with filament molecules arranged in a non-centrosymmetric pattern. The combination of TPEF and SHG therefore simultaneously provide structural information about different molecules at the same position [Liu et al., 2013a].

Intercalated Disc and Actin-Myosin Interaction May Regulate the Force on the Z-Disc

The local movement of cardiomyocytes during myofibril disassembly was analyzed using our lab-developed CIA. When the movement of particles around the cells is synchronized with the movement of adjacent cell edges, the movement of the local cell-culture-medium [represented by the arrows (Fig. 4)] reflects the movement of the nearby cell edge, and will be kept in the matrix mainly to visualize the cell local movement. The factors to shorten and to elongate the cardiomyocyte exert mechanical stress on the intercalated discs in opposite directions. The balance of force through intercellular connection at the cell ends maintains cardiomyocyte morphology. Breaking the intercalated discs may remove the pulling effects exerted by the other cardiomyocytes and result in imbalance of forces at the cell ends, which induces irreversible myofibril shortening. The generation of force imbalance and its effect on corresponding cell morphology is schematically described in Fig. 8. Single myofibrils are laterally connected by desmin to form myofibril bundles in cardiomyocytes connected by intercalated discs. The ends of the myofibril bundles are connected to desmosome and fascia adherens junctions in intercalated discs through desmin and actin filaments, respectively [Sheikh et al., 2009]. Through these connections, the arrangement and structure of myofibrils in one cardiomyocyte are stabilized by the cardiomyocyte at the other side of the intercalated disc. Broken or damaged intercalated discs and the interaction of actin–myosin combine to induce an imbalance among the forces exerted on the intercalated disc and the adjacent Z-discs and the desmin network.

Conclusion

This study suggests that intercalated discs and actin–myosin interaction play an important role in maintaining the integrity of myofibrils by keeping a balance of the forces exerted at the cell ends.

Materials and Methods

Isolation and Culture of Cardiomyocytes from Adult Rats

Cardiomyocytes were harvested from adult Sprague–Daw-ley rats (4–8 weeks) according to a protocol approved by the University of Cincinnati Institutional Animal Care and Use Committee. The procedure conforms to the Guide for the Care and Use of Laboratory Animals published by the US National Institutes of Health (NIH Publication No. 85-23, revised 1996). The procedure for isolation of cardiomyocytes was modified from the previous description [O'Connell et al., 2007]. The animals were heparinized (50 units/100 g animal, i.p.) and then sacrificed by overdose of anesthesia (Ketamine 8 mg/100 g animal weight, i.p.). The hearts were removed and perfused with Ca^{2+}-free perfusion buffer (mM)

(NaCl 113, KCl 4.7, KH_2PO_4 0.6 NaH_2PO_4 0.7, $MgSO_4$ 1.2, $NaHCO_3$ 12, $KHCO_3$ 10, HEPES 10, Taurine 30, BDM 10, Glucose 5.5) for 7 min followed by enzyme solution (collagenase 1.4 mg/mL, trypsin 8 unit/mL, neutral protease 0.2 unit/mL, $CaCl_2$ 50 μM) for 60 min. The heart tissue was minced into small pieces (<1 mm^3) and agitated gently with a pipette until most of the cells were isolated. Calcium reintroduction was performed by gradually increasing calcium concentration as follows (μM): 100, 200, 500, and 1000 at 15 min intervals.

Ca^{2+} -free-perfusion time was reduced from 7 to 2.5 min and the enzyme-perfusion procedure was reduced from 60 to 50 min to obtain intercalated disc-connected cardiomyocytes. Ventricles were cut into large pieces (~5 mm^3) and incubated at 37°C for 10 min with gentle swirling for 30 sec every 5 min. Then, the large pieces were minced into small pieces (<1 mm^3), and calcium was reintroduced gradually from 100 to 1000 μM.

Obtained cardiomyocytes were resuspended with Dulbecco's modified Eagle's medium containing 20% FBS and examined under an inverted microscope with an on-stage incubator (37°C). Cellular behavior was checked using a CCD camera connected to a computer. Then, cardiomyocytes were plated on laminin-coated coverglass or Petri dishes and mounted on a real-time imaging system (IncuCyte ZOOM, Essen Bioscience) that was placed in a conventional cell-culture incubator. The culture medium was carefully changed to remove any unattached cells after 5 h.

Length-Width Ratio Calculation and Analysis

The living adult cardiomyocytes were imaged daily during culture. Cells were randomly selected from the daily snapshot of the cell culture, $n = 96$ (Day 0), $n = 115$ (Day 1), $n = 110$ (Day 2), $n = 95$ (Day 3), $n = 104$ (Day 4), to more precisely demonstrate the distribution of cell morphology. The length (L) and width (W) of each selected cell were measured through ImageJ software, and the L/W value was calculated and plotted versus the culture time.

Western Blot

Proteins were extracted from the cardiomyocytes cultured at Day 1 and Day 4 and separated by electrophoresis in sodium dodecyl sulfate polyacrylamide gel. The α-actinin and MyHC were immunolabeled with antibodies, (including anti-α-actinin [Abcam] and anti-MyHC [eBioscience]) after being transferred to a polyvinylidene fluoride membrane, and then, the proteins were labeled with HRP-conjugated secondary antibodies and detected with Amersham ECL Plus™ Detection Reagents (GE) followed by exposure and image development.

Immunohistological Staining

Cardiomyocytes were fixed with 4% paraformaldehyde. After permeabilizing the cells using Triton X-100 and blocking the active sites in blocking solution (0.2% Triton X-100, 5% normal serum and 1% bovine serum albumin in phosphate buffered saline) for 30 min at room temperature, primary antibodies, including anti-α-actinin (Abcam), anti-connexin-43 (Santa Cruz), anti-MyHC (Abcam), anti-plakoglobin, and anti-desmin (Novus Biologicals) were applied. After being thoroughly washed, secondary antibodies (goat-anti-mouse and

goat-anti-rabbit) conjugated with FITC or Alexa-568 were applied. The labeled cells were then immersed in mounting solution containing DAPI and imaged under a fluorescence microscope. Sarcomeric structure was observed using our lab-built TPEF-SHG imaging system using a procedure similar to that in our previous report [Liu et al., 2013a]. Briefly, cells were excited by an 830-nm femtosecond laser beam, and the two-photon fluorescence signal emitted by the fluorescently labeled proteins was collected from the TPEF channel while the SHG signal from the myosin filaments was collected from the SHG channel. The TPEF and SHG signals were collected simultaneously and 2D images were processed and reconstructed using ImageJ software (http://rsbweb.nih.gov/ij/) and edited in MicrosoftV® Paint.

Local Cell-Movement Analysis

The local movement of cardiomyocytes during myofibril disassembly was analyzed using our lab-developed CIA. The high-speed CIA was built by connecting a monochrome high-speed CCD camera (Basler scA640-70gm, 70fps) to an inverse Olympus microscope combined with an onstage incubator. The high-speed video of the contracting cells acquired by the CCD camera was stored and processed by another computer connected to the camera through a gigabit ethernet cable. Each local feature on the cell image was recognized as a geometric point. The displacement of each point, which was used to visualize the local motion, was estimated through a cross-correlation analysis of two consecutive frames using a plugin for ImageJ software (https://sites.google.com/site/qingzongtseng/piv) [Tseng, 2011; Tseng et al., 2012]. Direction of the movements are represented by the colored arrows; distances of the movements (time interval = 71 ms) are represented by both arrow length and color of the arrows.

Statistical Analysis

The shape of cardiomyocyte was collected from 45 randomly selected areas at each time point (3 cardiomyocyte isolations, 3 samples/isolation, 5 areas/sample). Other data were obtained from at least three repetitions of experiment. The quantitative data were expressed as mean ± SEM and analyzed by Student's *t*-test and a P-value < 0.05 was accepted as a significant difference.

Supplementary Material

Refer to Web version on PubMed Central for supplementary material.

Acknowledgments

This work was supported by the National Institutes of Health (HL114654 and HL105176 to M. X., P20RR021949 to B. Z. G.). We are grateful to Christian Paul, at the Department of Pathology and Laboratory Medicine, University of Cincinnati Medical Center, for generously sharing his expertise in manuscript writing and discussion.

References

Ahuja P, Perriard E, Perriard JC, Ehler E. Sequential myofibrillar breakdown accompanies mitotic division of mammalian cardiomyocytes. J Cell Sci. 2004; 117:3295–3306. [PubMed: 15226401]

Asimaki A, Tandri H, Huang H, Halushka MK, Gautam S, Basso C, Thiene G, Tsatsopoulou A, Protonotarios N, McKenna WJ, et al. A new diagnostic test for arrhythmogenic right ventricular cardiomyopathy. N Engl J Med. 2009; 360:1075–1084. [PubMed: 19279339]

Atherton BT, Meyer DM, Simpson DG. Assembly and remodelling of myofibrils and intercalated discs in cultured neonatal rat heart cells. J Cell Sci. 1986; 86:233–248. [PubMed: 3654777]

Bar H, Strelkov SV, Sjoberg G, Aebi U, Herrmann H. The biology of desmin filaments: how do mutations affect their structure, assembly, and organisation? J Struct Biol. 2004; 148:137–152. [PubMed: 15477095]

Engel FB, Schebesta M, Duong MT, Lu G, Ren S, Madwed JB, Jiang H, Wang Y, Keating MT. p38 MAP kinase inhibition enables proliferation of adult mammalian cardiomyocytes. Genes Dev. 2005; 19:1175–1187. [PubMed: 15870258]

Eppenberger HM, Zuppinger C. In vitro reestablishment of cell-cell contacts in adult rat cardiomyocytes. Functional role of transmembrane components in the formation of new intercalated disk-like cell contacts. Faseb J. 1999; 13(Suppl):S83–S89. [PubMed: 10352149]

Helmes M, Trombitas K, Granzier H. Titin develops restoring force in rat cardiac myocytes. Circ Res. 1996; 79(3):619–626. [PubMed: 8781495]

Kostin S, Hein S, Bauer EP, Schaper J. Spatiotemporal development and distribution of intercellular junctions in adult rat cardiomyocytes in culture. Circ Res. 1999; 85:154–167. [PubMed: 10417397]

Lin ZX, Eshelman JR, Forry-Schaudies S, Duran S, Lessard JL, Holtzer H. Sequential disassembly of myofibrils induced by myristate acetate in cultured myotubes. J Cell Biol. 1987; 105:1365–1376. [PubMed: 3654756]

Liu H, Shao Y, Qin W, Runyan RB, Xu M, Ma Z, Borg TK, Markwald R, Gao BZ. Myosin filament assembly onto myofibrils in live neonatal cardiomyocytes observed by TPEF-SHG microscopy. Cardiovasc Res. 2013a; 97:262–270. [PubMed: 23118131]

Liu HH, Qin W, Shao YH, Wang ZH, Yang HX, Runyan RB, Borg TK, Gao BZ. Disassembly of Myofibrils in Adult Cardiomyocytes during Dedifferentiation. Proceedings of SPIE: Imaging, Manipulation, and Analysis of Biomolecules, Cells, and Tissues XI. 2013b; 85871W 26 February 2013. doi: 10.1117/12.2005156.

McCain ML, Lee H, Aratyn-Schaus Y, Kleber AG, Parker KK. Cooperative coupling of cell-matrix and cell-cell adhesions in cardiac muscle. Proc Natl Acad Sci USA. 2012; 109:9881–9886. [PubMed: 22675119]

McKoy G, Protonotarios N, Crosby A, Tsatsopoulou A, Anastasakis A, Coonar A, Norman M, Baboonian C, Jeffery S, McKenna WJ. Identification of a deletion in plakoglobin in arrhythmogenic right ventricular cardiomyopathy with palmoplantar keratoderma and woolly hair (Naxos disease). Lancet. 2000; 355:2119–2124. [PubMed: 10902626]

Messerli JM, Eppenberger-Eberhardt ME, Rutishauser BM, Schwarb P, von Arx P, Koch-Schneidemann S, Eppenberger HM, Perriard JC. Remodelling of cardiomyocyte cytoarchitecture visualized by three-dimensional (3D) confocal microscopy. Histochemistry. 1993; 100:193–202. [PubMed: 8244770]

Nishii K, Morimoto S, Minakami R, Miyano Y, Hashizume K, Ohta M, Zhan DY, Lu QW, Shibata Y. Targeted disruption of the cardiac troponin T gene causes sarcomere disassembly and defects in heartbeat within the early mouse embryo. Dev Biol. 2008; 322:65–73. [PubMed: 18671960]

O'Connell TD, Rodrigo MC, Simpson PC. Isolation and culture of adult mouse cardiac myocytes. Methods Mol Biol. 2007; 357:271–296. [PubMed: 17172694]

Plotnikov SV, Millard AC, Campagnola PJ, Mohler WA. Characterization of the myosin-based source for second-harmonic generation from muscle sarcomeres. Biophys J. 2006; 90:693–703. [PubMed: 16258040]

Previs MJ, Beck Previs S, Gulick J, Robbins J, Warshaw DM. Molecular mechanics of cardiac myosin-binding protein C in native thick filaments. Science. 2012; 337(6099):1215–1218. [PubMed: 22923435]

Saffitz JE. The pathobiology of arrhythmogenic cardiomyopathy. Annu Rev Pathol. 2011; 6:299–321. [PubMed: 21073337]

Sepp R, Severs NJ, Gourdie RG. Altered patterns of cardiac intercellular junction distribution in hypertrophic cardiomyopathy. Heart. 1996; 76:412–417. [PubMed: 8944586]

Sequeira V, Nijenkamp LL, Regan JA, van der Velden J. The physiological role of cardiac cytoskeleton and its alterations in heart failure. Biochim Biophys Acta. 2014; 1838:700–722. [PubMed: 23860255]

Sheikh F, Ross RS, Chen J. Cell-cell connection to cardiac disease. Trends Cardiovasc Med. 2009; 19:182–190. [PubMed: 20211433]

Simpson DG, Decker ML, Clark WA, Decker RS. Contractile activity and cell-cell contact regulate myofibrillar organization in cultured cardiac myocytes. J Cell Biol. 1993; 123:323–336. [PubMed: 8408216]

Thiene G, Nava A, Corrado D, Rossi L, Pennelli N. Right ventricular cardiomyopathy and sudden death in young people. N Engl J Med. 1988; 318:129–133. [PubMed: 3336399]

Tseng, Q. Study of Multicellular Architecture with Controlled Microenvironment. Université de Grenoble. (in French). 2011. Available at: https://tel.archives-ouvertes.fr/tel-00622264/

Tseng Q, Duchemin-Pelletier E, Deshiere A, Balland M, Guillou H, Filhol O, Thery M. Spatial organization of the extracellular matrix regulates cell-cell junction positioning. Proc Natl Acad Sci USA. 2012; 109:1506–1511. [PubMed: 22307605]

Zhou J, Shu Y, Lü SH, Li JJ, Sun HY, Tang RY, Duan CM, Wang Y, Lin QX, Mou YC, Li X, Wang CY. The spatiotemporal development of intercalated disk in three-dimensional engineered heart tissues based on collagen/matrigel matrix. PLoS One. 2013; 8:e81420. [PubMed: 24260578]

Abbreviations used

ARVC	arrhythmogenic right ventricular cardiomyopathy
CIA	contractile imaging assay
FBS	fetal bovine serum
LRS	long rod shape
MyHC	myosin heavy chain
RS	round shape
SRS	short rod shape
TPEF–SHG	two-photon excitation fluorescence-second-harmonic generation

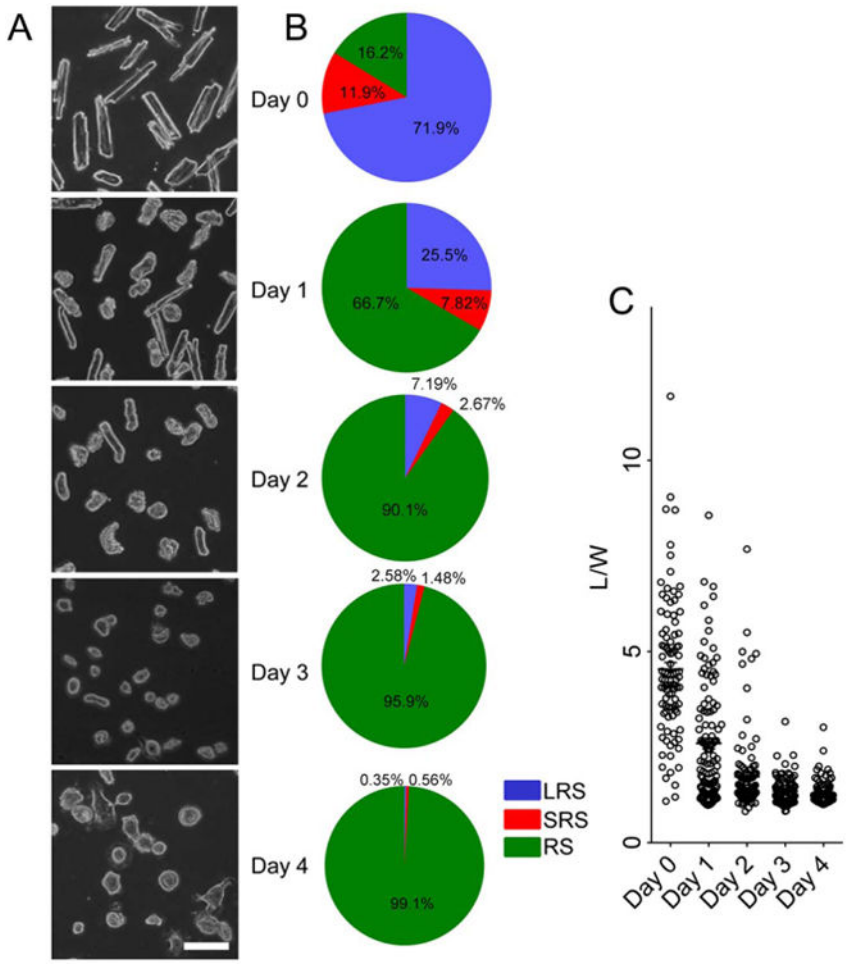

Fig. 1. Morphology of adult cardiomyocytes at different culture stages

(**A**) Snapshots of the cardiomyocytes cultured from Day 0 to Day 4. Scale bar: 100 μm. (**B**) Ratio of the cardiomyocytes of different morphologies. LRS: Long rod shape, SRS: short rod shape, RS: round shape. (**C**) Distribution of L/W at each time point. Each dot denotes the L/W value of a single cell.

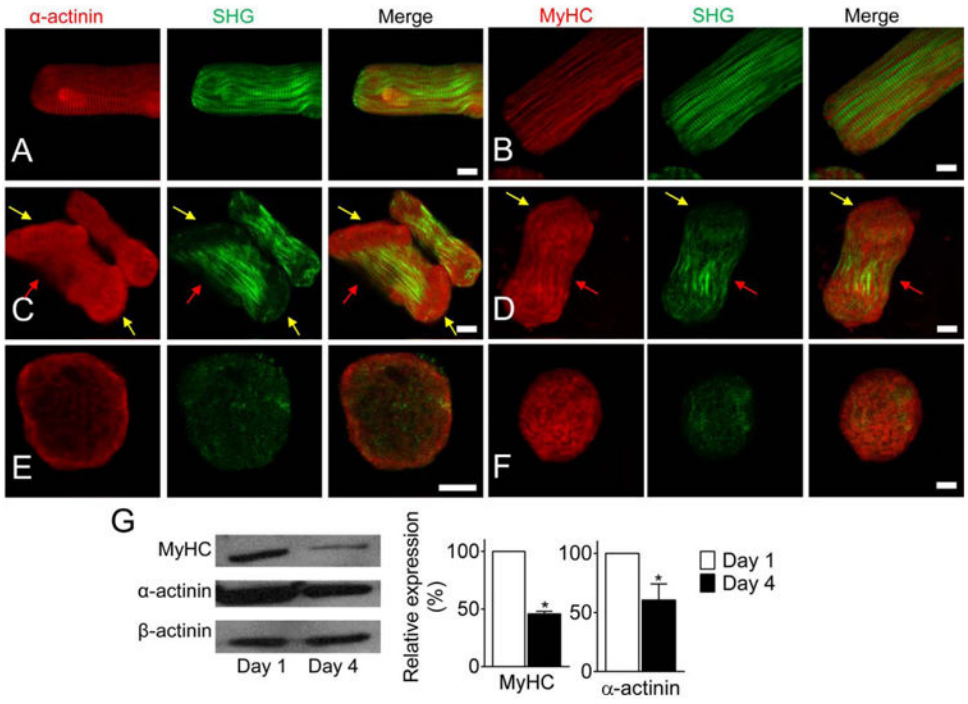

Fig. 2. Disassembly of myofibrils in cultured single adult cardiomyocytes

(**A-B**) LRS cardiomyocytes with clearly striated α-actinin, MyHC, and myofibril (SHG). (**C-D**) Myofibrils were disassembled from the cell ends in peanut-shape cells. α-actinin accumulated at the end of cells (yellow arrows), striated Z-discs disappeared, and myosin filaments broke up. But MyHC molecules were still detected at the cellular regions. The striated structure was still visible at the middle region (red arrows). (**E-F**) myofibrils had totally disassembled in the RS cardiomyocytes. α-actinin accumulated at the cell periphery and MyHC randomly aggregated in the cell. (**G**) Western blot and semi-quantitative data of MyHC and α-actinin in cardiomyocytes cultured Day 1 and Day 4, respectively. * $P < 0.05$, compared with Day 1. Scale bar: 10 μm.

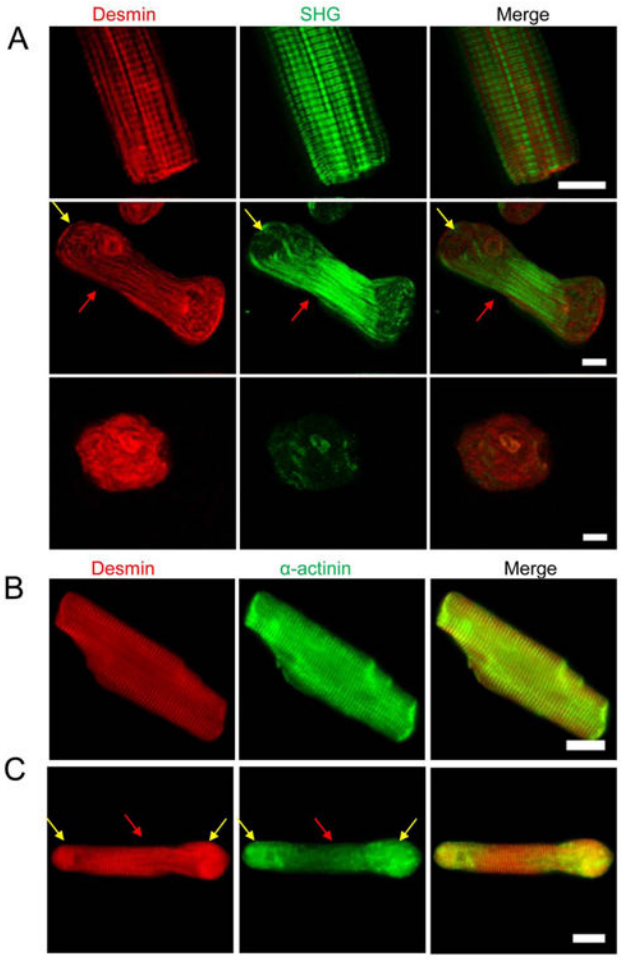

Fig. 3. Desmin network and myofibril release from myofibril bundles

(**A**) The patterns of desmin in the different shapes of cardiomyocytes. The striated pattern was still visible at the middle region (red arrows), but disappeared at the ends of a peanut-shape cell (yellow arrows). (**B**) Striated myofibril structure is clearly shown in a LRS cardiomyocyte, and the patterns of desmin and α-actinin are co-localized. (**C**) The striated myofibril patterns disappeared at the cell ends (yellow arrows) and the patterns of desmin and α-actinin became mismatched in peanut-shape cells. At the middle region of the cell (red arrows), the striated patterns of desmin and α-actinin are still visible and co-localized. Scale bar: 10 μm.

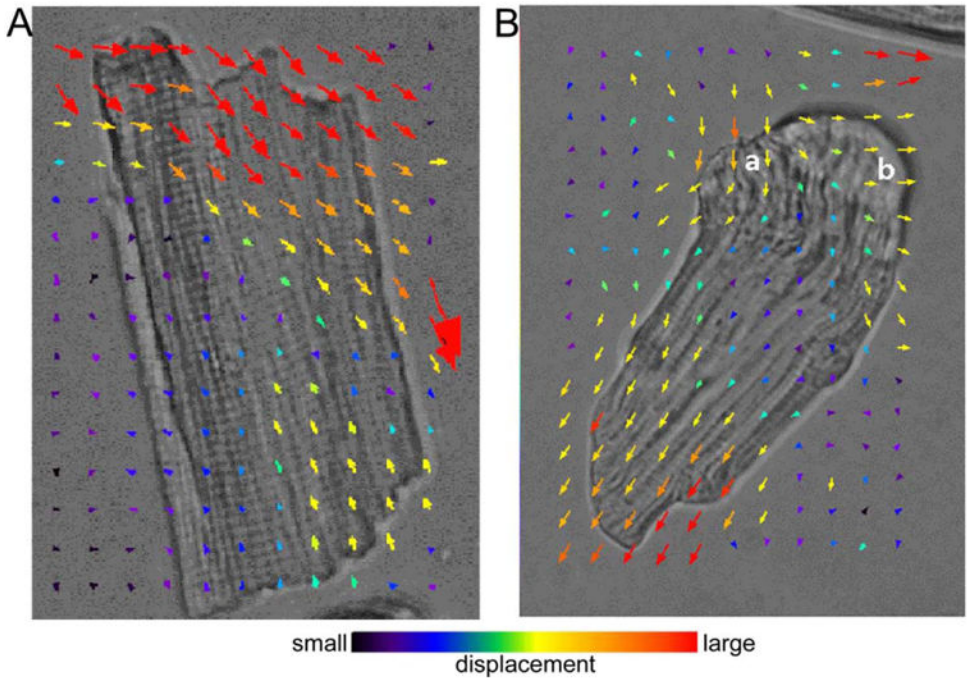

Fig. 4. Contractile image analysis of the cardiomyocyte components movements

(**A**) Before myofibril disassembly, movement during contraction of a cardiomyocyte (Supporting Information Video 1) was in the same direction. (**B**) The movement of a cardiomyocyte with single myofibrils at one end that have been released at areas a and b (Supporting Information Video 2) from the laterally bound myofibril bundles. The movement of cardiomyocyte components was uncoupled.

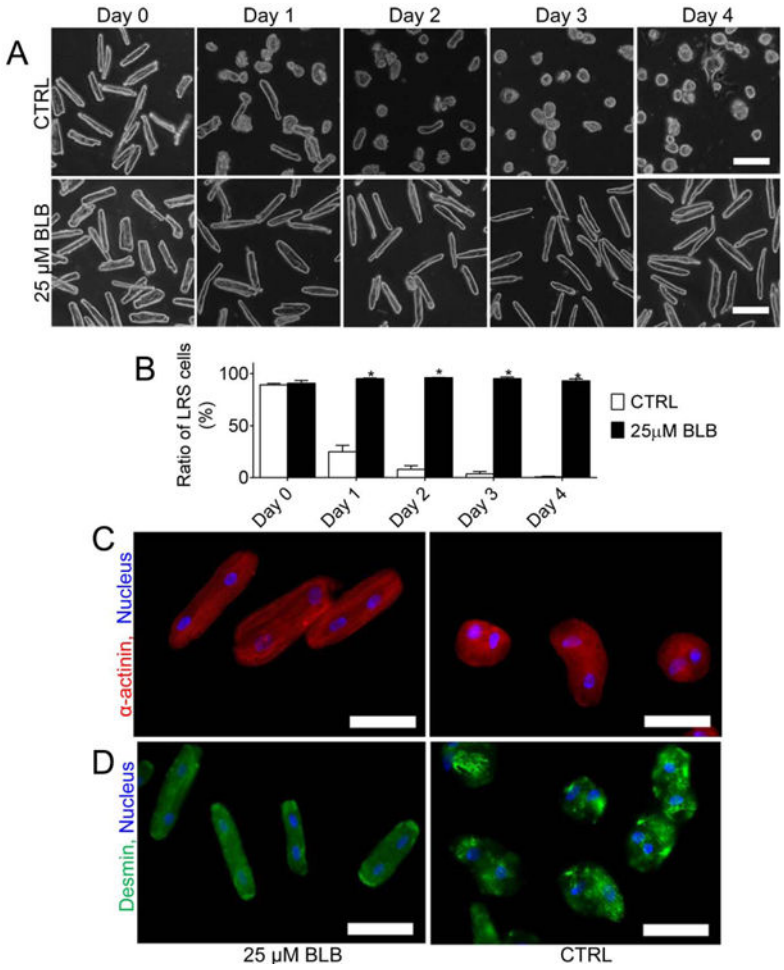

Fig. 5. Effect of actin–myosin interaction on morphology of adult cardiomyocytes

(**A**) Representative images of cardiomyocytes cultured in medium with or without 25 μM BLB at different time points (Day 0–4). Scale bar: 100 μm. (**B**) The percentage of LRS cardiomyocytes. *, $P < 0.05$ versus Control. (**C-D**) BLB maintained the distribution of α-actinin and preserved desmin and myofibril structure. Scale bar: 50 μm. CTRL: control, BLB: Blebbistatin.

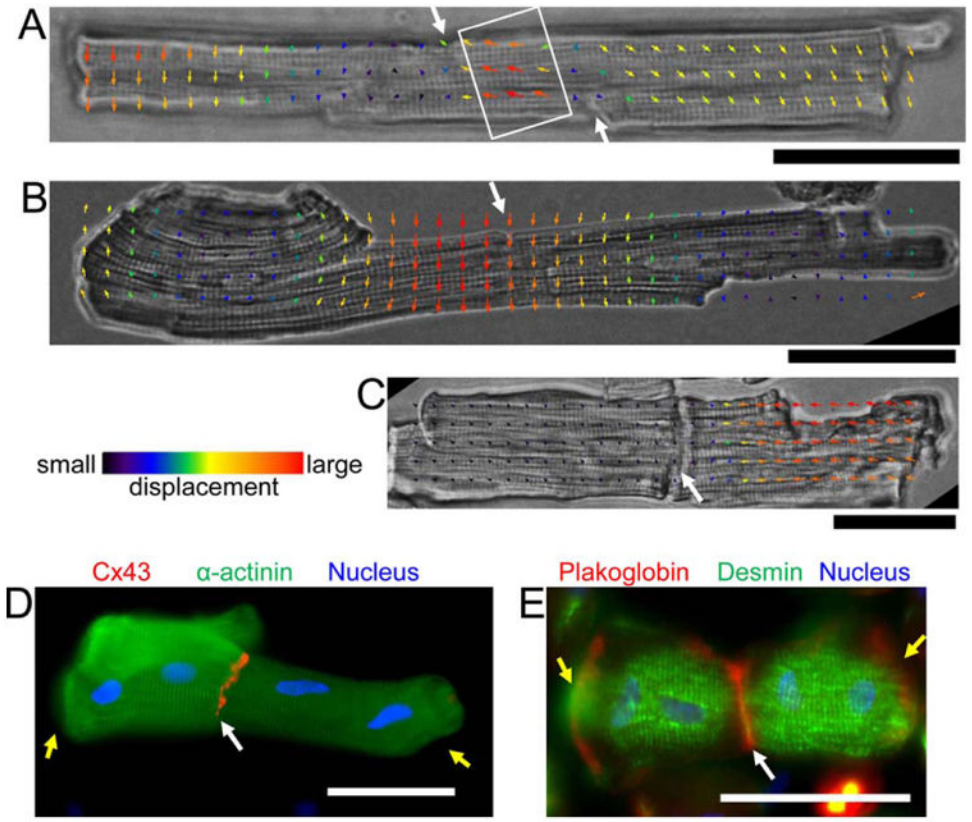

Fig. 6. Effect of intercalated discs on movement of cultured adult cardiomyocytes

(**A**-**C**) Freshly isolated cardiomyocytes connected through intercalated discs. (A) and (B) Cardiomyocytes with well-preserved intercalated discs. (C) Cardiomyocytes with damaged intercalated discs. The local movement in the cardiomyocytes was analyzed using contractile image analysis. (A-B) Contraction wave (white rectangle in A) in both cardiomyocytes was well-synchronized at the intercalated discs (white arrows). Similar local displacement fields at each side of well-preserved intercalated discs (B). Completely different local displacement fields at each side of damaged intercalated discs (C). (**D**-**E**) The cardiomyocytes (Day 1) were double stained with α-actinin (green) and connexin 43 (C×43) (red) (D), desmin (green) and plakoglobin (red) (E), respectively. Blue: nucleus. Yellow arrows indicate disassembly of myofibrils at the cell ends. Scale bar: 50 μm.

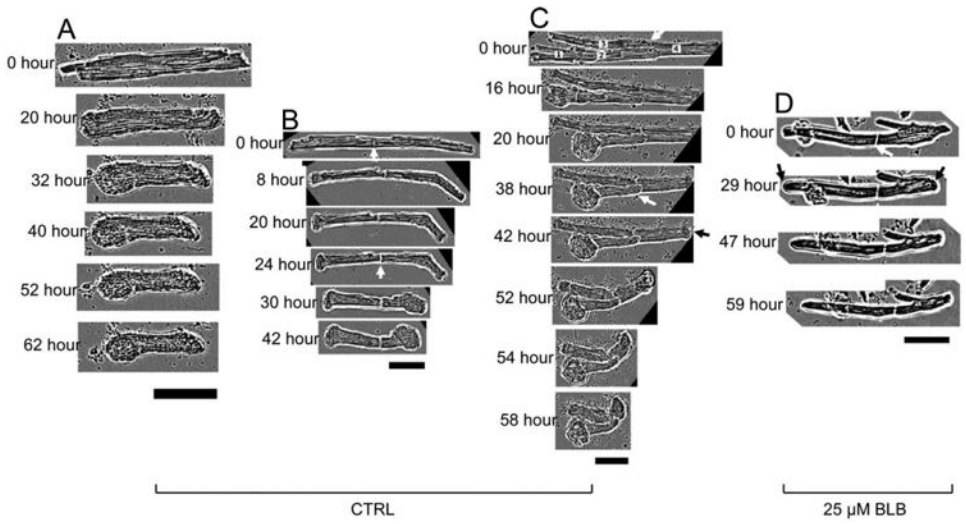

Fig. 7. The real-time morphology of cardiomyocytes with intercalated discs

(**A-C**) Cardiomyocytes cultured in medium that did not contain BLB. (A) Both ends of a single cardiomyocyte rapidly became peanut-shape. (B) Free ends of the cardiomyocytes with intercalated discs became peanut-shape rapidly. (C) Multiple cardiomyocytes connected through intercalated discs; each cardiomyocyte was labeled with numbers at 0 h. (**D**) Cardiomyocytes cultured in medium containing 25 μM BLB; the morphology of the whole cell was generally preserved. White arrows: the intercalated discs. Black arrows: the round cell ends. Scale bars: 50 μm. CTRL: control, BLB: Blebbistatin.

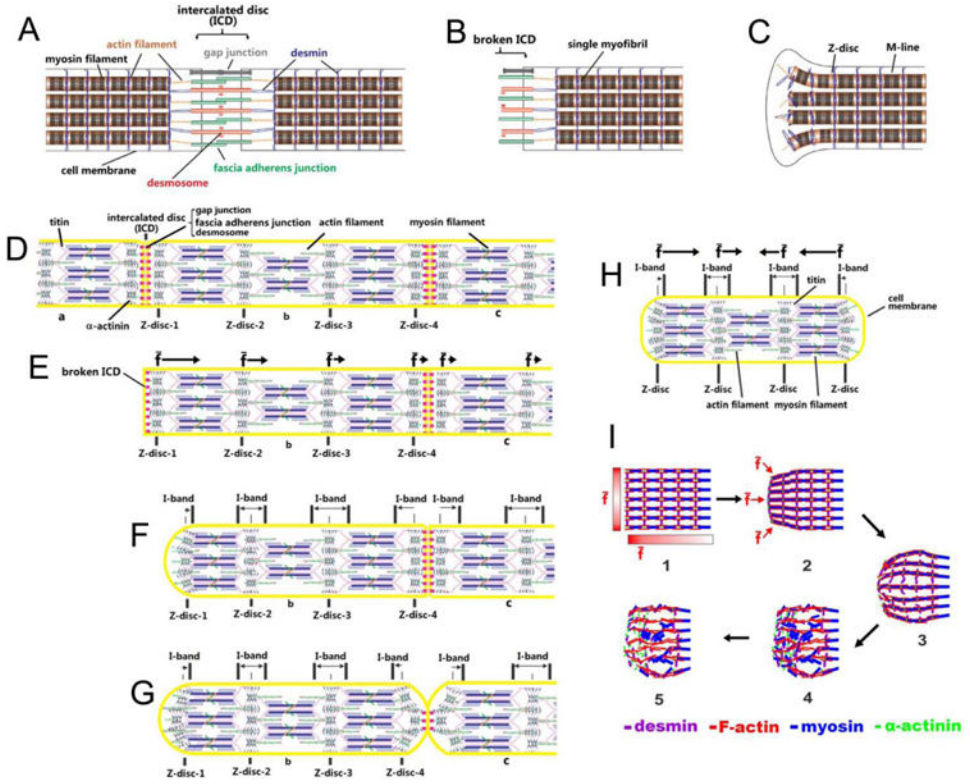

Fig. 8. Schematic description of the generation of force imbalance and the disassembly of myofibrils at the end of isolated adult cardiomyocytes

(**A**) Cardiomyocytes connected by untouched intercalated discs. (**B**) Cell end with broken intercalated disc. (**C**) Contraction of single myofibrils unbinds the myofibril bundles and releases single myofibrils, making the cell's free end wider than its middle region (peanut-shape). (**D**) The simplified structure of three cardiomyocytes, labeled a, b, and c, connected end-to-end through intercalated discs. The forces experienced by the Z-discs (Z-disc 1–4) in cell-b are balanced during continuous beating. (**E**) Complete breakage of the intercalated disc through removal of cell -a induces force imbalance on the Z-discs (Z-disc 1–4) in cell-b. The overlap of pulling forces induced by the actin–myosin interaction makes the time-averaged resultant force ($\bar{f}$) exerted on the Z-discs close to the left end stronger than that on the Z-discs far from the left end in cell-b. The direction and strength of $\bar{f}$ is indicated by the black arrows. (**F**) The force imbalance causes the left end of cell-b to shrink and become round. (**G**) Partial break of the intercalated disc between cell-b and -c causes partial shrinkage of the cell ends. (**H**) The shrinkage of both ends of a single isolated cardiomyocyte. (**I**) The process of morphological change and myofibril disassembly induced by force imbalance at one end of an isolated cardiomyocyte. The time sequence of each step is indicated by black arrows. The red gradient bars (Step 1) indicate the strength of the time-averaged resultant force ($\bar{f}$) at different positions of the cell end. The darker gradient bar region represents stronger $\bar{f}$ at the corresponding position. The direction of $\bar{f}$ at the corresponding position is indicated by red arrows in Step 2.